

## ELECTRONIC SUPPLEMENTARY MATERIAL

### Development of a Two-Stage Model System to Investigate the Mineralization Mechanisms Involved in Idiopathic Stone Formation: Stage 2- *In Vivo* Studies of Stone Growth on Biomimetic Randall's Plaque

Allison L. O'Kell,<sup>1,2</sup> Archana C. Lovett,<sup>3</sup> Benjamin Canaeles,<sup>1</sup> Laurie B. Gower,<sup>3</sup> Saeed R. Khan<sup>1,4</sup>

<sup>1</sup> Department of Urology, College of Medicine, University of Florida, Gainesville, FL

<sup>2</sup> Department of Small Animal Clinical Sciences, College of Veterinary Medicine, University of Florida, Gainesville, FL

<sup>3</sup> Department of Materials Science & Engineering, University of Florida, Gainesville, FL

<sup>4</sup> Department of Pathology, College of Medicine, University of Florida, Gainesville, FL

Corresponding authors: Saeed R. Khan: [Khan@pathology.ufl.edu](mailto:Khan@pathology.ufl.edu)  
Laurie B. Gower: [LGower@mse.ufl.edu](mailto:LGower@mse.ufl.edu)

In addition to XRD data (Fig. S1), Figures S2 – S9 provide a more detailed perspective on the variety of morphologies found on and within the BRP-induced CaOx “stones” produced with ethylene glycol treatment. The figures are organized to illustrate common features that were observed, and particularly those attributes deemed relevant to formation mechanisms. Possible mechanistic clues derived from the *ex vivo* images are described, although the discussion is speculative given that “stone” formation obviously could not be monitored *in situ*, and one cannot know exactly what species were present in the urine during the CaOx overgrowths. The interested reader may want to watch for our follow-up paper which describes some similar morphological features that were observed in our *in vitro* model system, which in that setup provides the ability to examine formation mechanisms *in situ*, and under precisely controlled conditions.

#### **Supplementary Figures:**

**Fig. S1** X-ray diffraction (XRD) of crystals from the “normal water” specimens.

**Fig. S2** Representative examples overall morphologies of BRP-induced CaOx “stones” from each of the 4 BRP-EG groups.

**Fig. S3** Fracture surfaces of BRP-induced “stones” showing transition in textures from internal BRP core, to disorganized CaOx aggregates, to dense smooth exteriors.

**Fig. S4** Closer examination of organic material at the surface of “biomimetic stones”.

**Fig. S5** Examination of organic material within the interior of “biomimetic stones”, but which does not resemble the organic matrix of the underlying BRP core, and thus deposited as the stone was forming.

**Fig. S6** COD stability in BRP “stones”.

**Fig. S7** Transitions from amorphous granular to radial growth patterns.

**Fig. S8** Mixed COM textures in a BRP-induced “stones” that may lead to radial outgrowths.

**Fig. S9** Proclivity of stacked COM aggregates to grow into compact, spherically-bound morphologies.

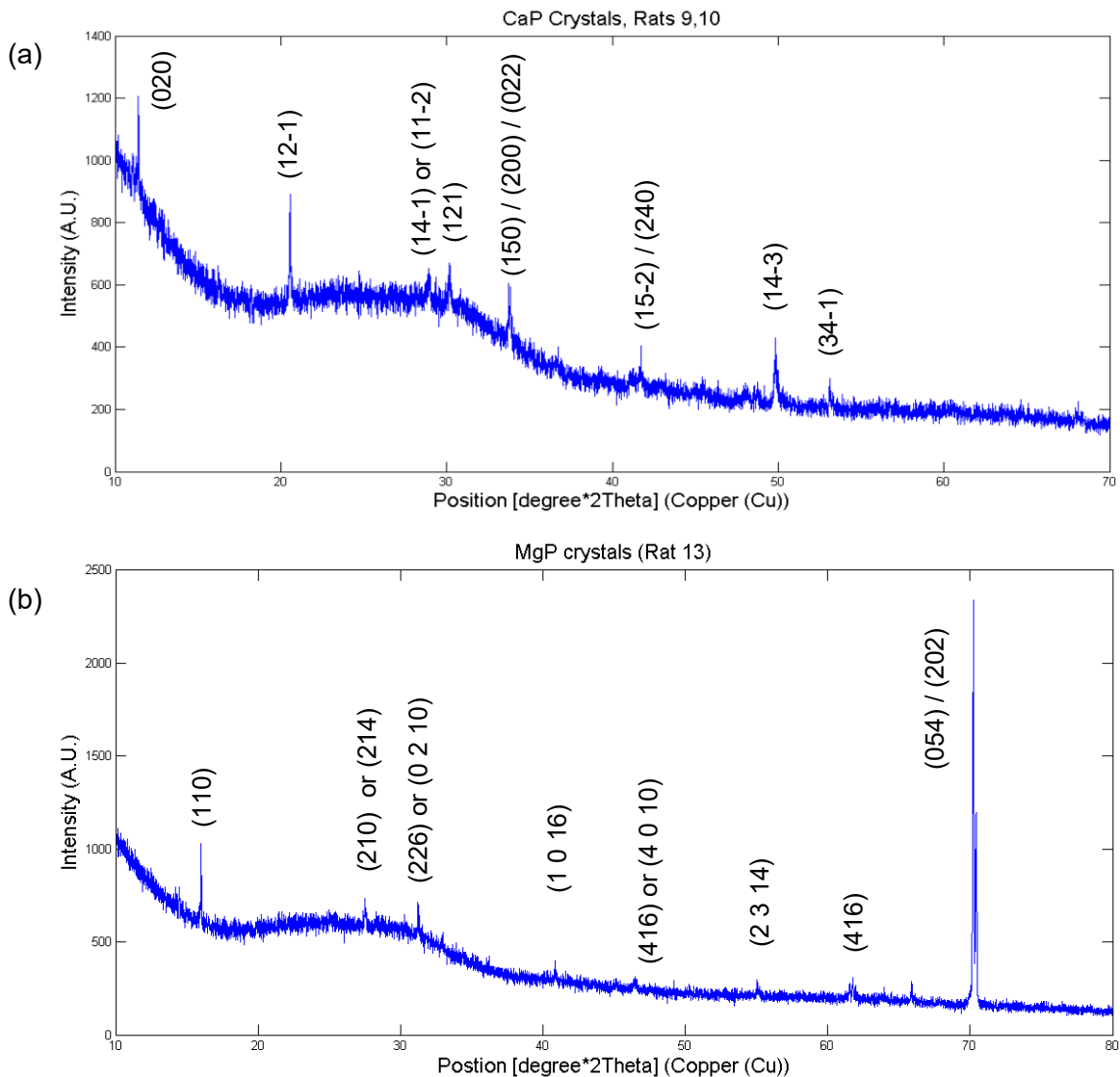


**Fig. S1** X-ray diffraction (XRD) of crystals from the “regular water” specimens. (a) The top XRD pattern was from the crystals shown in Figure 4c-d (BRP-C group, normal water). The peak assignments shown above are based on reference pattern matching<sup>1-3</sup>, and suggests the crystals are most likely brushite (dicalcium phosphate dihydrate). The pattern lacks the often prominent (040) peak, but this is consistent with other reports of aqueous grown brushite.<sup>3</sup> (b) The bottom XRD pattern was from the crystals shown in Figure 5b (BRP-PA, normal water), which had the same morphology as those in Figure 5c-d (BRP-OPN group, normal water). The peak assignment software found a closest match to calcium-magnesium hydrogen phosphate in one obscure paper,<sup>4</sup> but it only went to a 2-theta of 60°. We could find no other literature on this phase, but a couple of papers on Mg-containing apatite phases also seem to suggest that this is some type of Mg-CaP phase.<sup>5-6</sup>

1. Kuznetsov VN, Yanovska AA, Stanislavov AS, Danilchenko SN, Kalinkevich AN, Sukhodub LF (2016) Controllability of brushite structural parameters using an applied magnetic field. *Materials Science and Engineering C* 60:547–553
2. Mandel S, Tas AC (2010) Brushite ( $\text{CaHPO}_4 \cdot 2\text{H}_2\text{O}$ ) to octacalcium phosphate ( $\text{Ca}_8(\text{HPO}_4)_2(\text{PO}_4)_4 \cdot 5\text{H}_2\text{O}$ ) transformation in DMEM solutions at 36.5 °C. *Materials Science and Engineering C* 30:245–254
3. Toshima T, Tafua RHM, Takemura Y, Fujita S, Chohji T, Tanda S, Li S, Qin GW (2014) Morphology control of brushite prepared by aqueous solution synthesis. *J. of Asian Ceramic Societies* 2:52-56
4. Otsuka, R.; Ito, A.; Nakamura, S.; Akao, M.; Aoki, H., (1988) *Iyo Kizai Kenkyusho Hokoku, Tokyo Ika Shika Daigaku*, 22, 23 – 30.
5. Kuwahara, H.; Al-Abdullat, Y.; Mazaki, N.; Tsutsumi, S.; Aizawa, T., (2001) Precipitation of Magnesium Apatite on Pure Magnesium Surface during Immersing in Hank's Solution. *Materials Transactions*, 42 (7), 1317-1321.
6. Ma, W. H.; Liu, Y. J.; Wang, W.; Zhang, Y. Z., (2015) Improved biological performance of magnesium by micro-arc oxidation. *Brazilian Journal of Medical and Biological Research*, 48, 214-225.

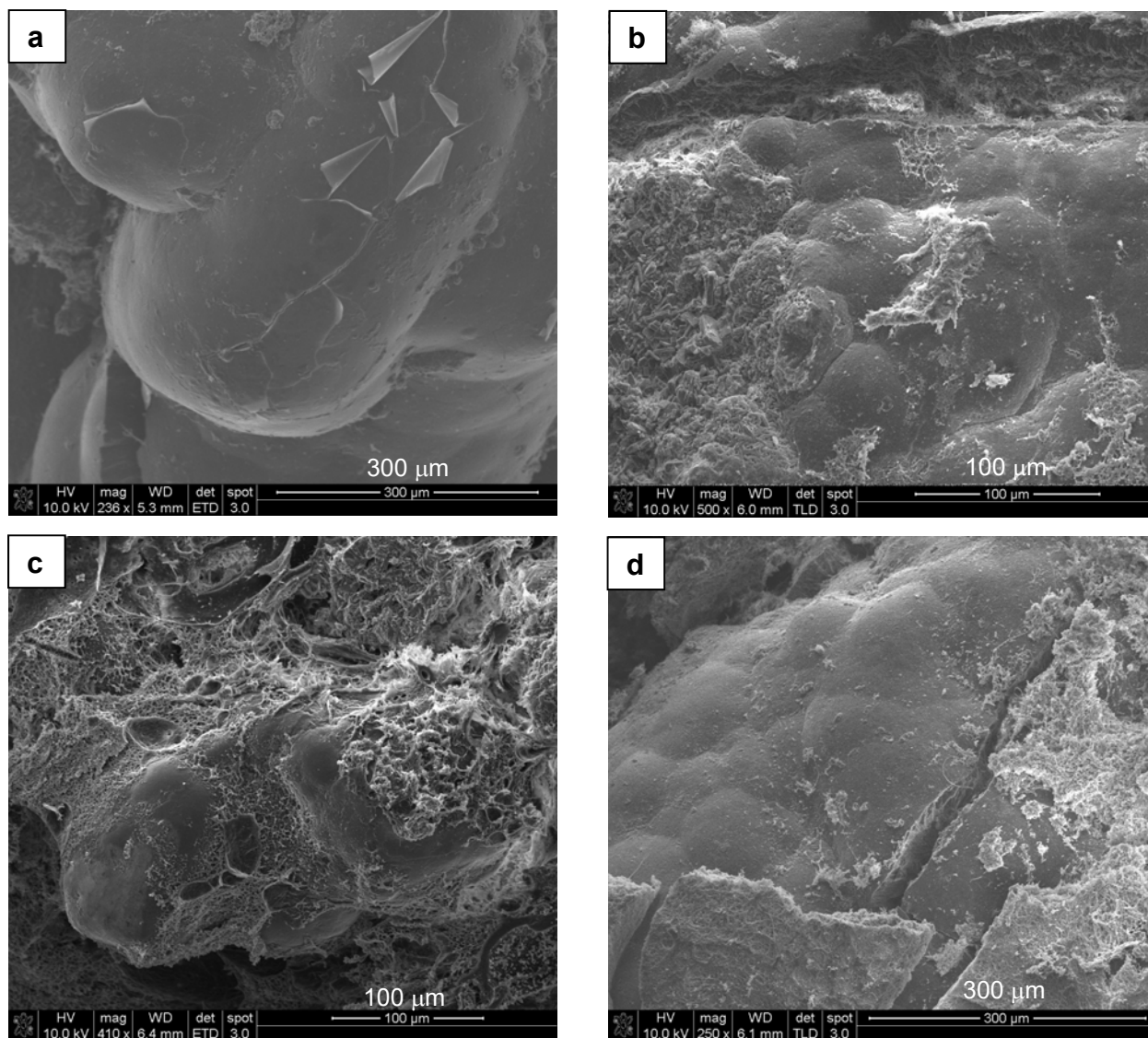


**Fig. S2** SEM micrographs showing representative examples of the outer surface and overall morphologies of BRP-induced CaOx “stones” from each of the 4 BRP-EG groups. Different surface textures (with variable amounts of adsorbed organics) are represented, but the different groups generally had examples (from one of the 4 rats) that would exhibit similar features. (a) BRP-PA stone with smooth rounded surfaces. A thin film-like coating of organic matter is peeling off, probably due to dehydration stress from SEM sample preparation. (b) BRP-C stone with smooth rounded regions on the right, but a rough region on the left with an accumulation of random CaOx aggregates. Clumps of organic matter are adsorbed on the smooth surfaces. (c) BRP-OPN stone, also with smooth rounded surfaces, along with a large clumps of organic matter smattered across different regions. (d) BRP-DNM stone with smooth rounded surfaces and a collection of thick mats of organic matter on the bottom and right sides.

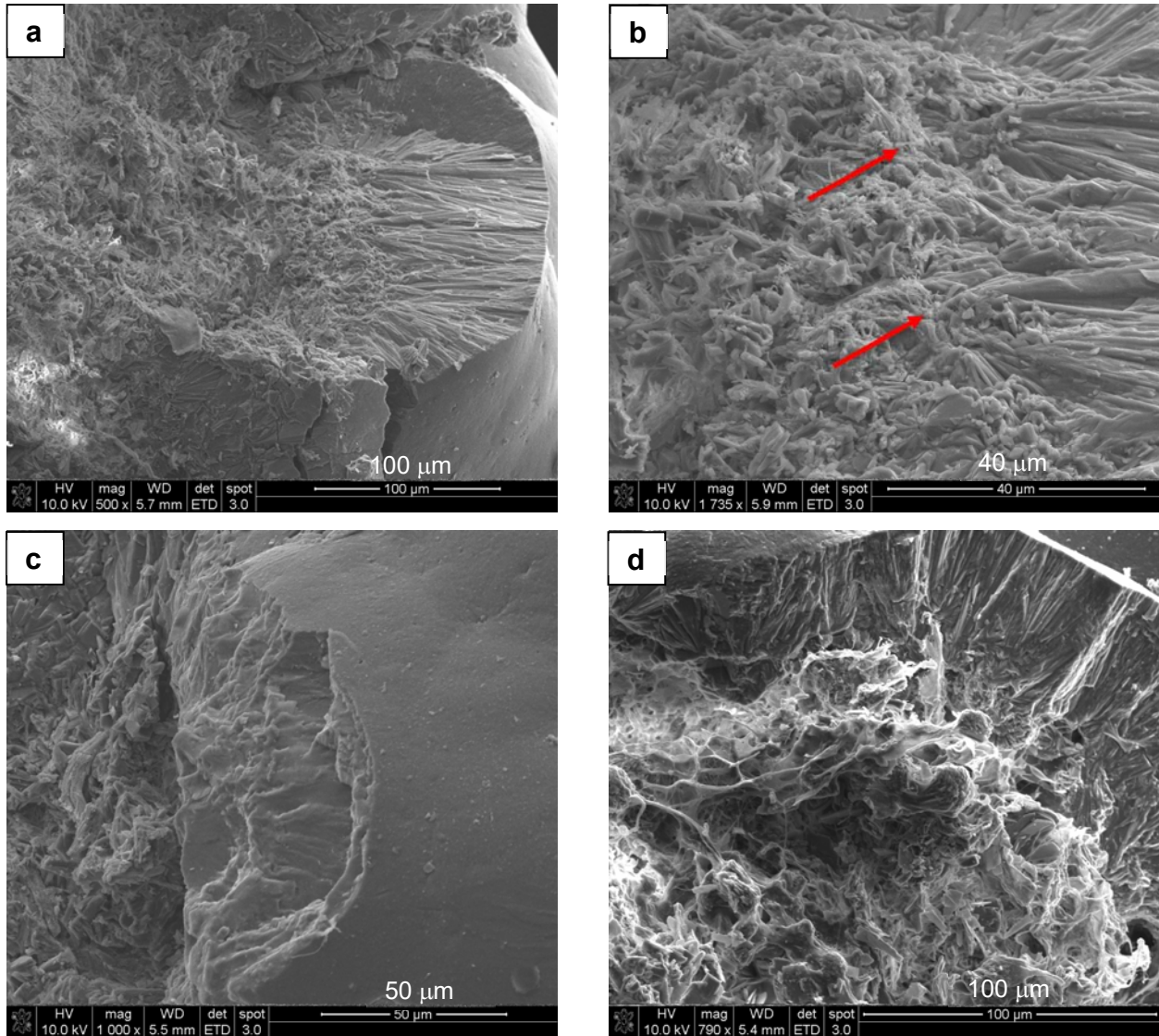


**Fig. S3** Fracture surfaces of BRP-induced “stones” showing transition in textures from internal BRP core, to disorganized CaOx aggregates, to dense smooth exteriors. These examples are all from BRP-PA, but similar features are seen in all BRP groups. (a) Fracture surfaces often exhibit an internal radial spherulitic texture that terminates with a smooth rounded surface (right), but which grows from a highly disorganized core (left). (b) Upon closer examination at higher mag. of the interfacial zone, some fibrous as well as granular material can be seen at or near the locations where radial crystallites emerge (arrows). (c) Concentric layering is sometimes seen within the spherulitic regions. (d) This example has a dense shell that grew fairly close to the underlying BRP substrate, but the dense radial crystals still seemed to have grown off of regions of disorganized CaOx aggregates embedded within the matrix.



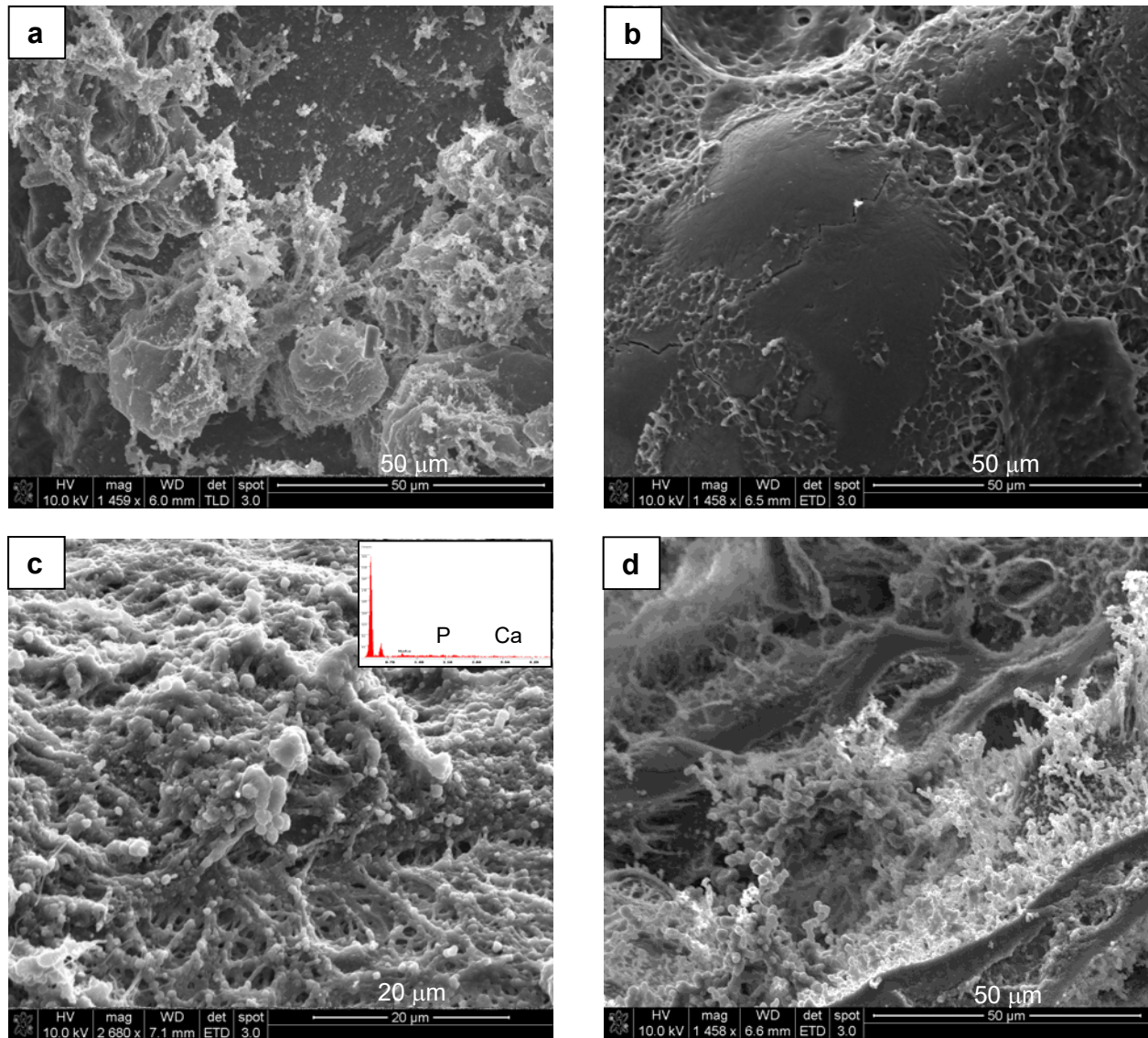


**Fig. S4** Closer examination of organic material at the surface of “biomimetic stones”. (a) This stone (from BRP-C) had a lot of surface coverage of organic material which accumulated in stacks. (b) Higher mag. of the stone shown in Fig. S1c (BRP-OPN) shows an organic coating with a dehydration pattern suggestive of a dehydrated hydrogel. (c) Fibrous organic matrix on a DNM-EG stone shows an accumulation of nodular clumps covering a fibrous matrix. The lack of Ca/P peaks in EDS (inset) indicates that these are not comprised of amorphous mineral. The broad range of nodule sizes suggests that these are not strands of bacteria or sloughed cells. (d) These nodular fibers appear to be growing upward off the substrate (bottom right). This example was from a BRP-OPN stone, but was seen in several samples when the fibrous matrix was not too thick and collapsed into stacks and sheets.

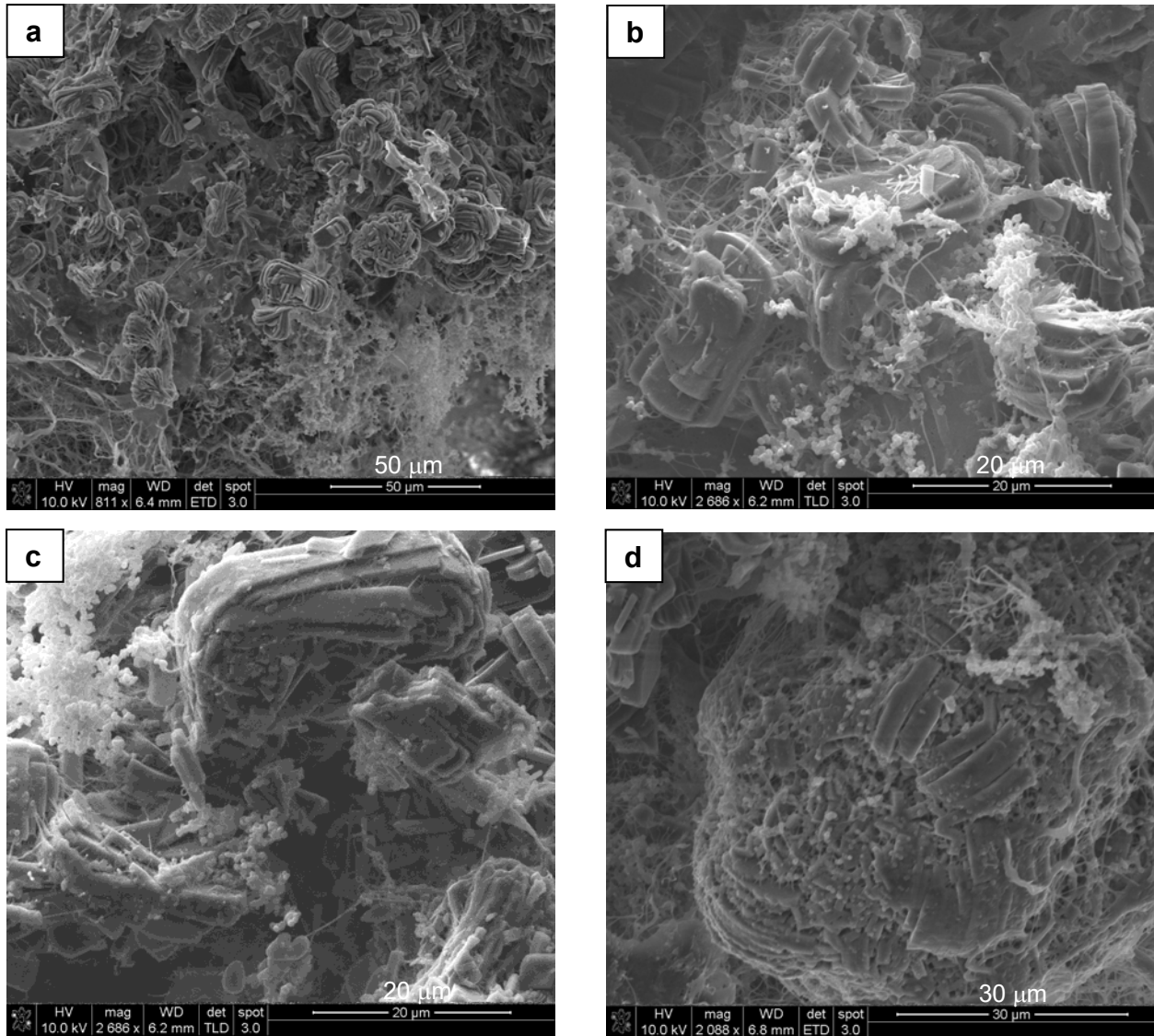


**Fig. S5** Examination of organic material within the interior of “biomimetic stones”, but which does not resemble the organic matrix of the underlying BRP core, and thus deposited as the stone was forming. (a) Large clump of nodular material amidst a region of layered COM dumbbells. The nodular matrix appears to be accumulating and hanging/growing off the substrate as fibers (BRP-OPN). (b) High magnification of a region with smaller clumps shows some underlying fine fibers that have not yet accumulated nodules, all of which are closely entwined with the mineral aggregates (BRP-DNM). (c) Similarly entwined mineral and organic phase, but with what appears to be an oddly bent crystal on the top aggregate (BRP-DNM). It is most likely the edge of underlying plate, which seem to grow with curved edges. (d) The organic matrix has become embedded between the crystals of a layered rosette (BRP-OPN).

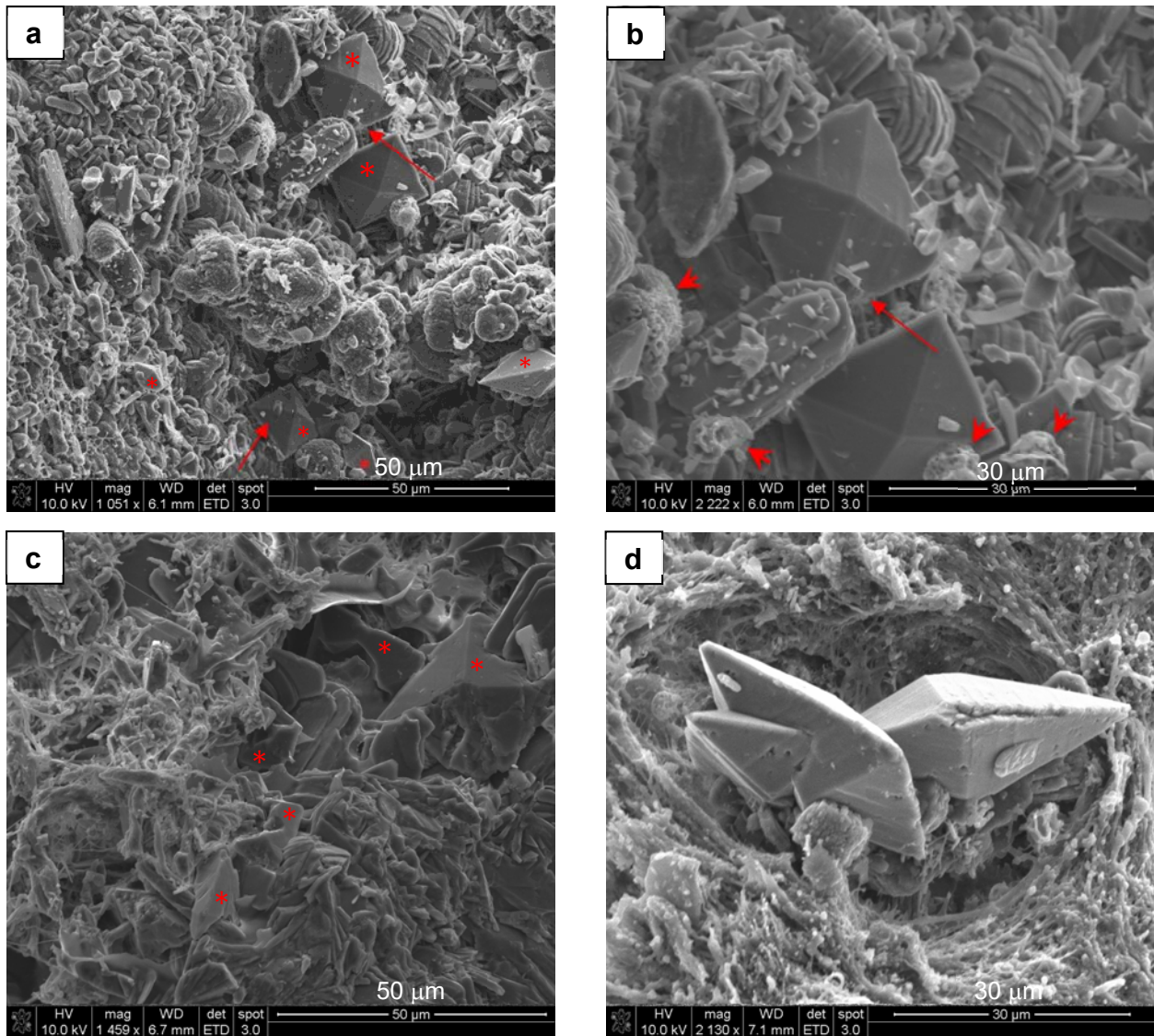


**Fig. S6** COD stability in BRP “stones”. Examples are from BRP-PA, except (d) is from BRP-DNM. (a) There are relatively few COD crystals amongst the many COM aggregates, but they are easily distinguished by their distinct bipyramidal habit (asterisks). Small pits are seen in two of the COD crystals (arrows). (b) Higher magnification of the pit on the top crystal shows small new crystals (presumably COM) emerging from the pits. A variety of other non-descript aggregates are also present, along with some porous entities (arrowheads), which may be undergoing dissolution-precipitation. (c) Several partially dissolved COD crystals (asterisks). COD is less stable than COM, so it is possible that there are often more COD crystals in the earlier stages that have subsequently undergone dissolution-precipitation into the COM phase. (d) COD crystals surrounded by nodular fibrous matrix, with dissolution pits and edges. Some overgrowths seem to be occurring on the bottoms of bipyramids.



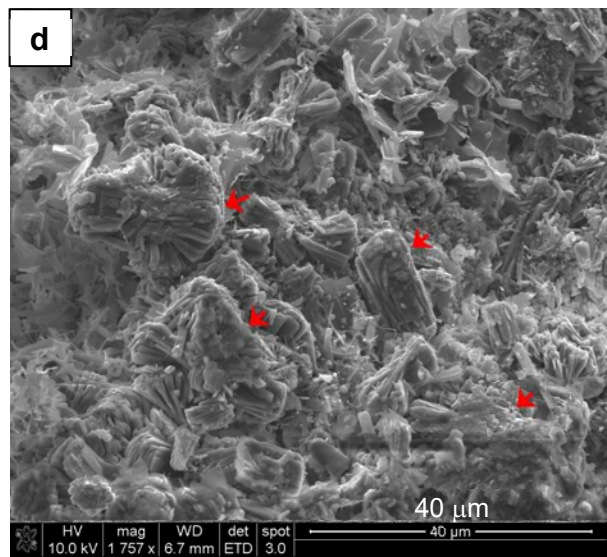
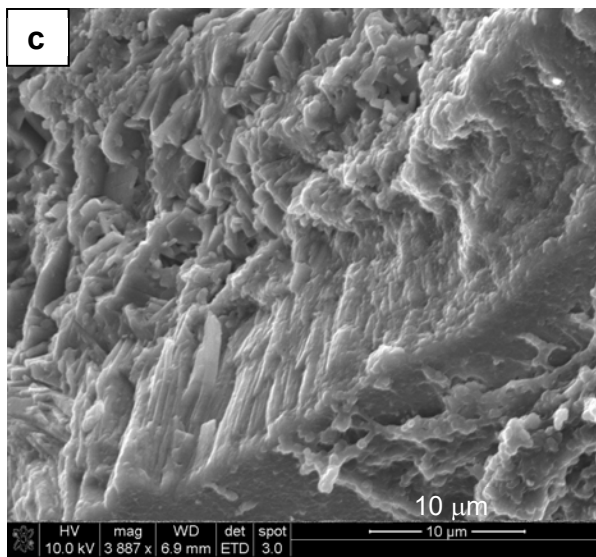
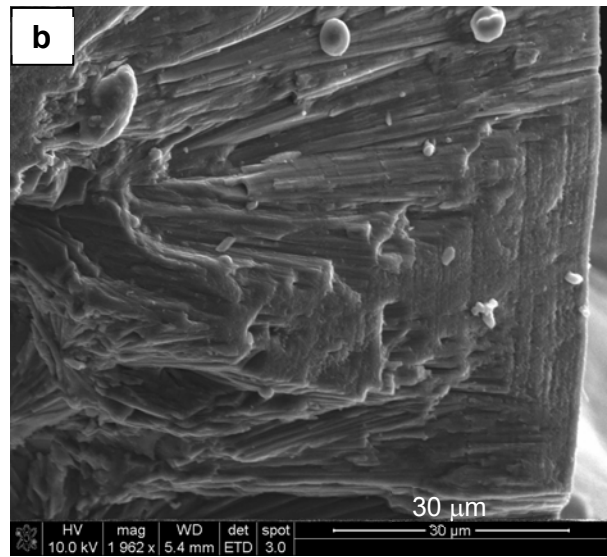
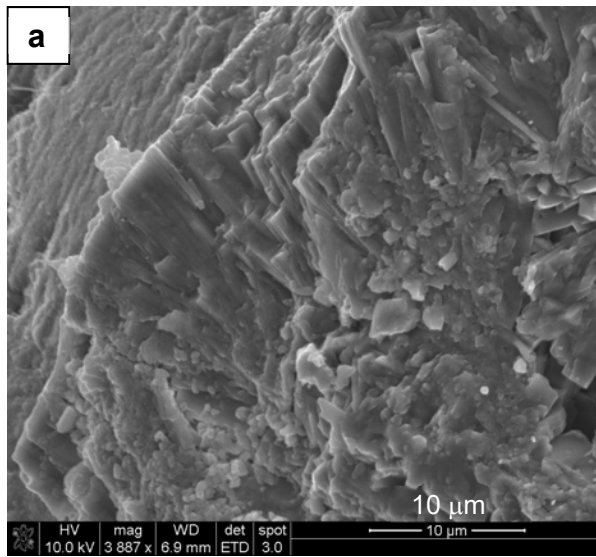


**Fig. S7** Transitions from amorphous granular to radial growth patterns. (a) Radial crystallites seem to emanate from a region containing granular amorphous matter (BRP-OPN). (b) The growth front termini of each layer in the central swath seem to exhibit a rough and granular texture (BRP-PA). (c) The bottom edge where the texture is just becoming radial shows a gradual transition from granular to smooth rods. The nodular fibers are seen melding into the bottom surface, which seem similar to the granular material surrounding this region. Although these nodular fibers are clearly organic in nature in the prior images, one gets the impression here that they are collecting amorphous mineral that is fusing into the growing spherulites (BRP-OPN). (d) First impressions would suggest this is just a random assortment of crystal aggregates within organic matrix, but when zooming in, one can see many regions of granularity where the crystals seem to be forming from amorphous substance (arrowheads).

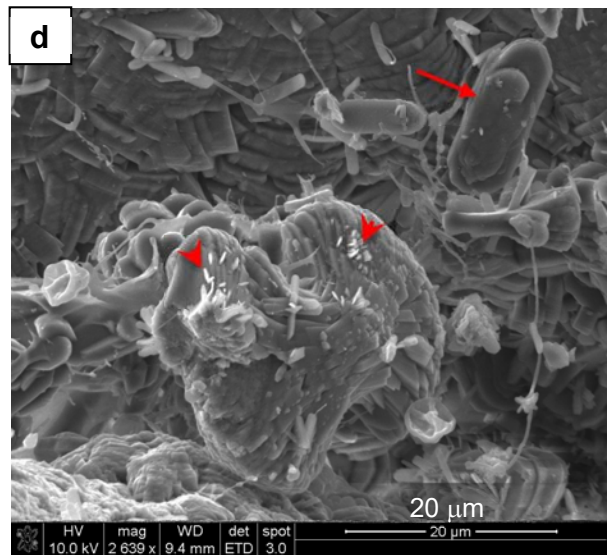
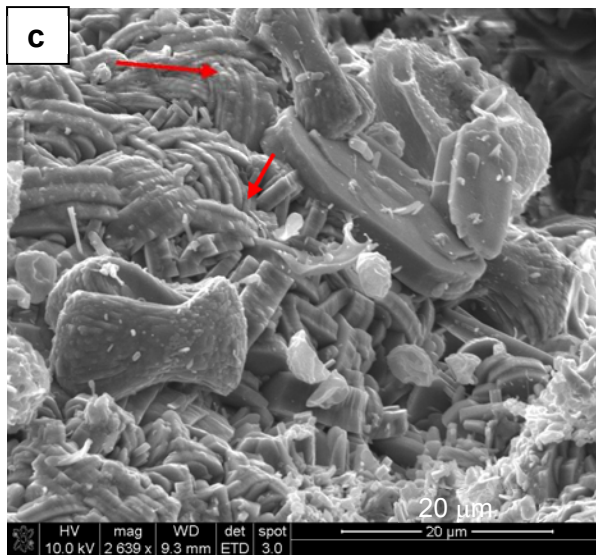
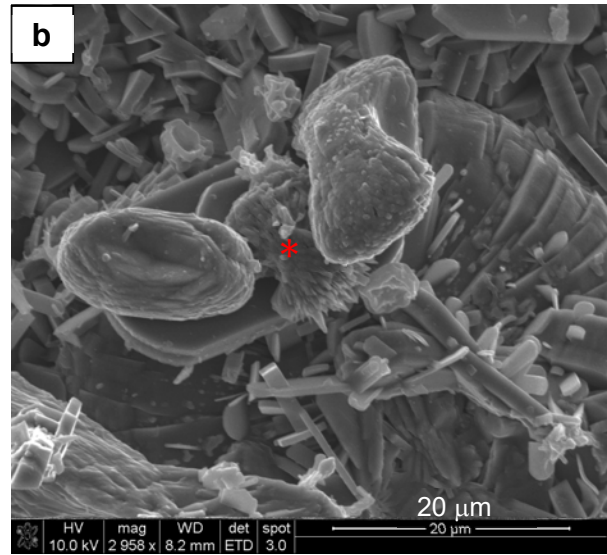
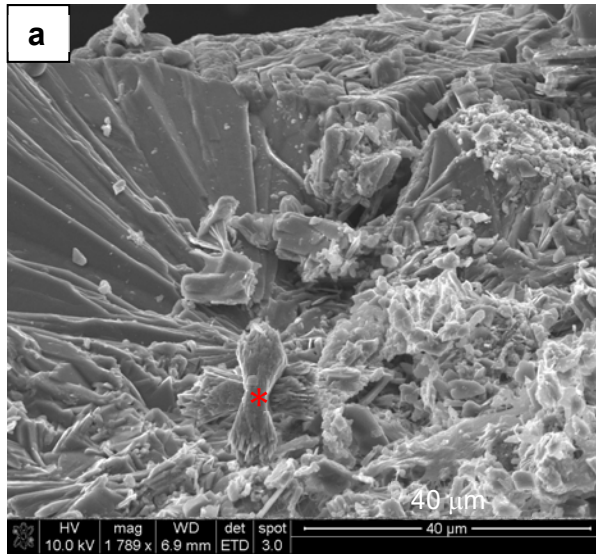


**Fig. S8** Mixed COM textures in a BRP-induced “stones” that may lead to radial outgrowths. These are from BRP-PA stones, but typical of all samples. (a) Large thick radial plates growing out of disorganized region. In this case, the radial growths appear to be a fracture surface that is oblique to the stacked plates to the right. However, near the center of the radiating plates are two small crisscrossed dumbbells (asterisk) with a finer texture than the layered dumbbells, and these have clear radial needle outgrowths. (b) The finer texture in these three dumbbells seems to result from a different twinning pattern, and the middle dumbbell (asterisk) appears to be leading to radial needle-like outgrowths (BRP-PA). (c) Amidst the thick plates and stacks, some finely textured dumbbells are seen here as well. The bumpy surface texture on these is similar to that seen on some of the wide edges of the thick stacked dumbbells (arrows), both of which might provide secondary nuclei that could also lead to radial outgrowths. (d) Secondary nucleation appears to be occurring on these fanned out dumbbells (arrowheads). These could be envisioned as a means for producing a high density of radiating outgrowths. Twinning on the top “coffin” (arrow) is likely to lead to a stacked dumbbell or rosette.

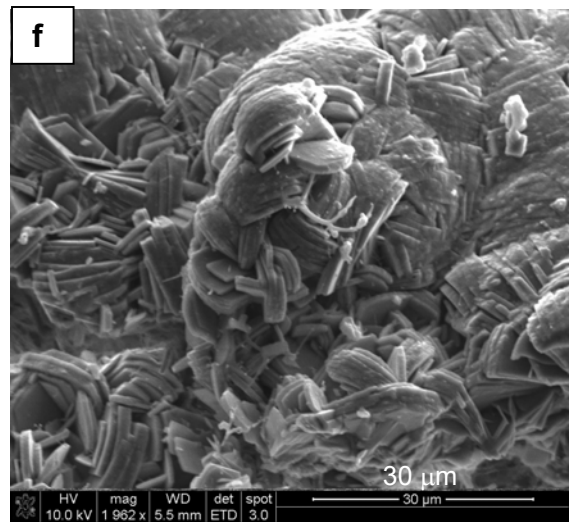
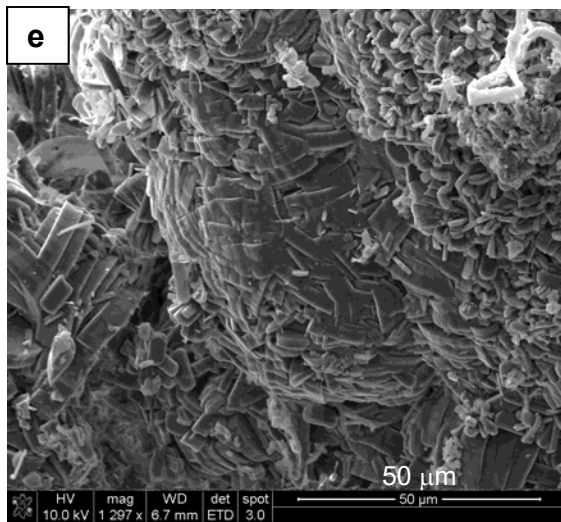
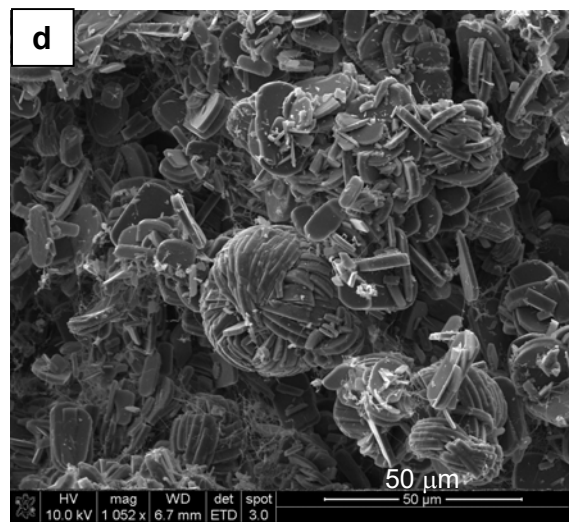
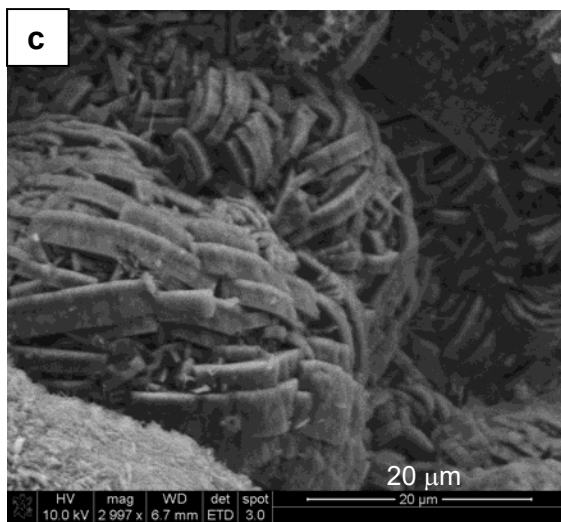
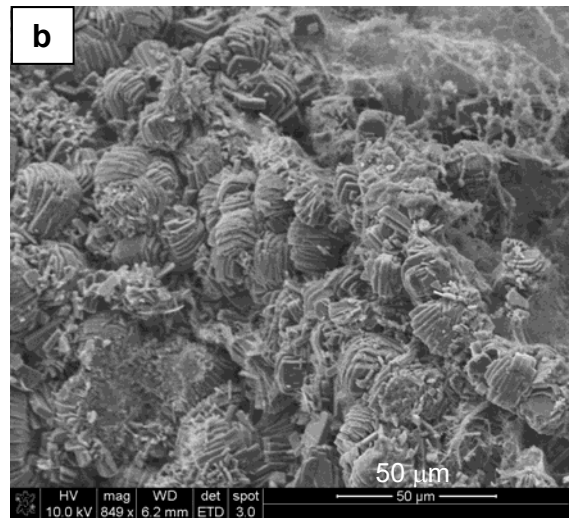
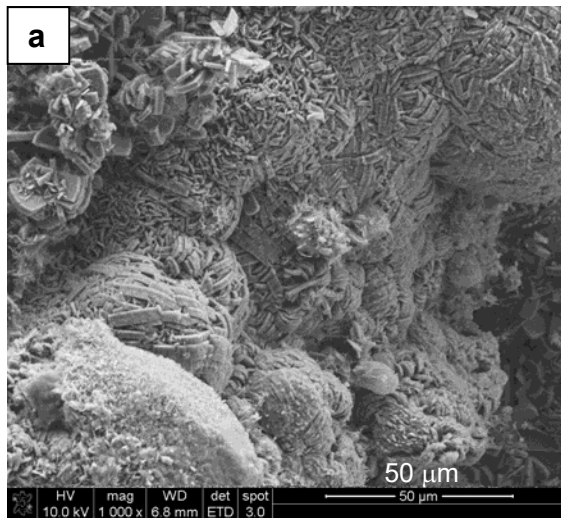


**Fig. S9** Proclivity of stacked COM aggregates to grow into compact, spherically-bound morphologies (a-c from BRP-DNM; d-f from BRP-OPN).